



ELSEVIER

1 June 1998

OPTICS
COMMUNICATIONS

Optics Communications 151 (1998) 413–421

Full length article

Motion control of ensembles of ordered optical vortices generated on finite extent background

D. Neshev¹, A. Dreischuh², M. Assa, S. Dinev³*Department of Quantum Electronics, Sofia University, 5, James Bourchier Blvd., BG-1164 Sofia, Bulgaria*

Received 23 October 1997; accepted 29 January 1998

Abstract

Vortex motion in ordered structures is analysed numerically in the frame of the 2D nonlinear Schrödinger equation. Analogies with superfluid dynamics are presented. It was found that coherent interaction of optical vortex solitons (OVSs) leads to vortex motion, which can be adequately described by the Kelvin law in superfluid dynamics for large offsets between the OVSs. Cancellation of motion in some spatial configurations of vortices and vortex lattices is observed. The possibility to steer the motion of vortex ensembles is discussed. © 1998 Elsevier Science B.V. All rights reserved.

PACS: 42.65.-k; 42.65.Sf; 42.65.Tg; 42.65.Wi

1. Introduction

The concept of wavefront-dislocations (edge, screw, or mixed edge-screw), along which the phase is undetermined and the field amplitude is zero, was introduced in the wave theory by Nye and Berry [1]. The point phase dislocations (in two dimensions) are also called vortices. Vortex formations are known from works on superfluid dynamics [2,3] and quantum mechanics [4], but they are a subject of recent interest in optics [5,6], especially for the generation of optical vortex solitons [7–10].

Optical vortices are characterized as localized intensity dips with two-dimensional screw phase dislocations, imposed on a bright background beam. From the mathematical point of view, such screw phase profile is described by the $\exp(im\varphi)$ multiplier, where φ is the azimuthal coordinate and m is an integer number whose sign determines

the direction of the dislocation. The counterclockwise direction is denoted as a positive Topological Charge (TC). Beams with such helical phase profiles can be generated in lasers with large Fresnel number cavities [11], by using helical phase plates [12], laser mode converters [13,14], by computer generated holograms [15,16] or as a result of instabilities of dark soliton stripes in Nonlinear Media (NLM) [17–19].

In a linear regime of propagation the optical vortex retains its phase portrait and the dark core does broaden, whereas in the absence of a helical phase distribution a Poisson spot does appear in the far-field power-density distribution. In the presence of defocusing nonlinearity the optical vortex can evolve into a two-dimensional spatial Optical Vortex Soliton (OVS). For the first time the existence of stable OVSs was predicted in Ref. [20] and experimentally demonstrated in Ref. [8]. The interest toward these self-supported dark beams is motivated by their inherent ability to induce gradient optical waveguides in the defocusing NLM. They can serve as steerable “conduits” information carrying beams/pulses and seem attractive for all-optical switching applications. The OVSs are found to be stable in a scalar nonlinear system [20] and unstable under perturbation when polarization of the beam

¹ E-mail: drg@phys.uni-sofia.bg² Present address: MPI für Quantenoptik, Institut für Laserphysik, Hans-Kopfermann-Strasse 1, Postfach 1513, D-85748 Garching (b. München), Germany.³ Present address: Technical University Graz, Institute of Experimental Physics, Petersgasse 16, A-8010 Graz, Austria.

is taken into account (except for beams with circular polarization) [21].

It was found that as a result of the free-space propagation of an array of optical vortices nested in a smooth background beam, their relative position does depend on the mutual disposition of the TCs within the ensemble [22–26]. When a pair of vortices with equal TCs is considered their relative positions as well as their positions within the host beam, are invariant upon propagation and vortices move rigidly. In contrast, a pair of vortices with opposite TCs attract each other. They can collide and annihilate [22]. It was shown [23], that in a linear regime amplification vortices are restless and move continuously.

When a pair of vortices propagates through a self-defocusing NLM, the vortices evolve into 2D dark OVSs and they can be forced to rotate around the beam centre up to 180°. This rotation can be controlled by the beam intensity and/or material nonlinearity because both of them are able to alter the wavefront curvature thus modifying the relative position of the OVSs at the output plane [16]. This behaviour can be used for constructing rotary switches able to link an input port to an array of output ports.

Topological-stable patterns consisting of identically-charged vortices are modeled on the basis of the complex Ginzburg-Landau equation with space-dependent coefficients [27]. It is shown that the gradients of the complex coefficients can counterbalance the repulsion between the vortices, but spatial instability is claimed for spatially-independent coefficients.

The Nonlinear Schrödinger Equation (NLSE) could be considered as a special kind of Ginzburg-Landau equation with spatially-independent coefficients. It is shown [25,28] that for large intervortex separation the dynamics of vortices satisfying the cubic NLSE correspond to point vortex dynamics in an ideal two-dimensional fluid.

In this paper we investigate the evolution and robustness of ensembles of optical vortices and prove the possibility to stabilize (in space) ordered structures of OVSs in homogeneous and isotropic bulk Kerr self-defocusing nonlinear media. Indications for the possibility to achieve an all-optically controlled switching are found, when an array of input ports is rotary linked to an array of output ports. The eventual all optical control of the ensemble evolution may open the way toward future parallel switching devices based on OVSs. However we will not discuss the particular technical aspects.

2. Numerical analysis and tests

The evolution of dark subbeams imposed on a bright background beam in self-defocusing NLM is described by the (2 + 1)D NLSE:

$$i \frac{\partial A}{\partial z} + \frac{1}{2L_{\text{Diff}}} \nabla_{\perp}^2 A - \frac{1}{L_{\text{NL}}} |A|^2 A = 0, \quad (1)$$

for the slowly varying amplitude A of the electric field, where

$$\nabla_{\perp}^2 = \frac{\partial^2}{\partial \xi^2} + \frac{\partial^2}{\partial \eta^2} = \frac{1}{r} \frac{\partial}{\partial r} + \frac{\partial^2}{\partial r^2} + \frac{1}{r^2} \frac{\partial^2}{\partial \varphi^2}$$

is the transverse Laplacian and (ξ, η) ((r, φ)) are the dimensionless Cartesian (polar) coordinates, normalized to the dark beam radii. In Eq. (1), L_{Diff} and L_{NL} are the corresponding diffraction and nonlinear lengths. The latter are equal for a soliton mode of propagation.

Further to our previous analyses on incoherent OVSs interactions [29], presently we are interested in investigating the evolution of coherent superposition of such solitons. Eq. (1) is solved numerically by means of a 2D generalization of the split-step Fourier method with a grid mesh expanded over 2048 × 2048 points. In order to ensure conditions, under which undesired interaction between the axially offset OVSs and the finite background beam is negligible [30] we consider the vortex ensemble as imposed on a super-Gaussian beam of HWHM more than 20 times larger than the minimum of the OVS radii:

$$B(r) = \exp\left[-(r/w)^{12}\right], \quad w \geq 20. \quad (2)$$

When multiple vortices are imposed on the same background beam the initial field is considered as a product of the core functions of each vortex (see for example Eq. (19) in Ref. [25] or Eq. (4) in Ref. [26]). Exact-form solution for the core function does not exist but a convenient approximation used in our simulations is given by a tanh profile, which has a well defined core size (see for example Eq. (2) in Refs. [25,26] and Eq. (6) in Ref. [31]). In practise a beam with such core function can be formed with good accuracy using computer-generated holograms [15,16].

In order to proof the fidelity of our numerical procedure, we consider first the known nonlinear motion of a pair of OVSs [9,16,25] along the NLM. The coherent interaction of vortices, resulting in a pure nonlinear motion [9] (when vortices are imposed on a plane wave background) should be distinguished from the vortex motion at the focused background beam [16] (when the Guoy shift is responsible for rotation of the OVSs with equal TCs).

In both situations mentioned above and in agreement with Refs. [9,16,25], rotation of OVSs of equal TCs is observed, in contrast to the case of opposite TCs. In the second case a well expressed saturation of the rotation velocity with increasing input intensity is found.

In the case of a pure nonlinear rotation (when background beam focusing is absent) we did not observe any saturation of the rotation speed versus input intensity. It is found [9], that vortex motion in this case is very similar to the vortex motion in superfluids [2], where the nonzero

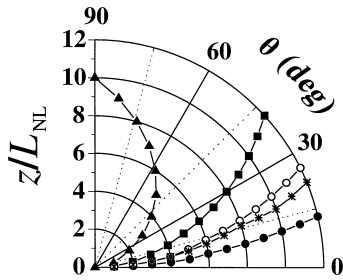


Fig. 1. Polar plot of the OVS pair (of equal TCs) rotation angle versus normalised nonlinear propagation path-length (solid circles – $\Delta=10.0, m=1$; open circles – $\Delta=10.0, m=2$; stars – $\Delta=7.5, m=1$; squares – $\Delta=5.0, m=1$; triangles – $\Delta=2.5, m=1$). Solid curves – best fits.

velocity (caused by the presence of other additional vortices) is given by the Kelvin law:

$$\frac{d\mathbf{r}_i}{dz} = \gamma \sum_{j \neq i} \frac{\mathbf{m}_j \times (\mathbf{r}_i - \mathbf{r}_j)}{|\mathbf{r}_i - \mathbf{r}_j|^2}. \quad (3)$$

In Eq. (3), $\mathbf{r}_{i,j}$ are the spatial positions of the vortices in the (x, y) plane and \mathbf{m}_j are vortex TC vectors in the direction perpendicular to the (x, y) plane. γ is a scale coefficient (in units of dimensionless length).

In Fig. 1 a polar plot of OVSs rotation angle θ versus normalized the nonlinear propagation path-length for different offsets $|\mathbf{r}_i - \mathbf{r}_j|$ at equal TCs is presented. The open circles presents the generalized case of interaction of vortices with TC $m=2$. It is clearly seen that the rotation in this case is twice faster than for the case of interacting unit-charged vortices of the same separation (solid circles). In all cases this rotation possesses a constant angular velocity.

The main feature in the propagation of OVSs with higher-order TCs is their instability. It was found [32] that multi-charged vortices (in the framework of the NLSE) are metastable, i.e. they possess soliton features but they are unstable under the influence of perturbation [1,31–34] and do decay into vortices with unit circulations.

The detailed analysis of the observed rotation confirmed that the OVS motion is adequately described by Eq. (3), which in the practical case of a vortex pair of equal TCs is transformed to the relation:

$$\frac{d\theta}{dz} = \gamma \frac{2m}{\Delta^2}, \quad (4)$$

where Δ is the mutual offset between the two vortices, and m stands for their TCs (assumed to be equal). To match the rotation of the OVSs to the rotation of the vortex lines in the superfluid dynamics (Eqs. (3), (4)) we obtained that the scale coefficient γ should be equal to 0.97 [dimensionless lengths]. (If the angle θ in Eq. (4) is measured in

degrees $\gamma = 55.4$ [deg \times dimensionless lengths].) In this way the superfluid theory describes quantitatively well the motion of the OVSs. Deviation from this dependence could be observed for small offsets ($\Delta < 5.0$) between the OVSs, which exerts the presence of polynomial dependence (of higher order) on Δ in the denominator of Eq. (4).

For pairs of vortices with opposite TCs, no rotation along the NLM is observed. The only motion is the shift of the vortex pair away from the background beam centre [9]. Such a characteristic behaviour was observed in our test experiments, when the background beam with dark subbeams nested in (generated by computer synthesized holograms) passed trough a cell, containing thermal self-defocusing NLM ('nujol', Merck). The measurements were performed with an experimental setup similar to that described in Ref. [35] (see also Ref. [8]) but with holograms for generating the optical vortices [16,26,33].

3. Vortex motion and stabilization of vortex ensembles

When a coherent superposition of more than two OVSs is considered, the detailed analysis of the numerical data presented bellow indicates that symmetrical structures consisting of N OVSs with equal TCs always rotate around the geometrical centre of the ensemble. This behaviour is well described by the superfluid dynamics approximation (Eq. (3)). Substituting the geometrical parameters of different symmetrical structures in Eq. (3) one can obtain the

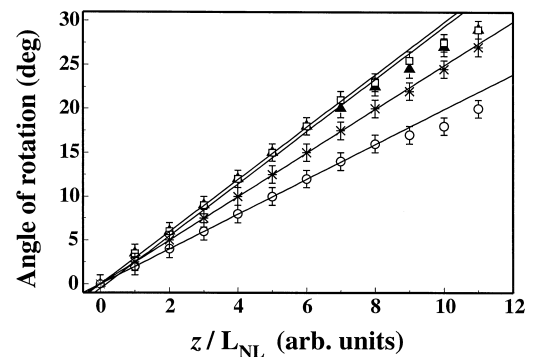


Fig. 2. Plot of the ordered OVS structure (of equal TCs) rotation angle versus normalised nonlinear propagation path-length (circles correspond to the vortex pair, triangles to the triangular form ensemble, squares to the square form ensemble, stars to the hexagonal form ensemble). The offset between the neighbouring OVSs is $\Delta=7.5$. Solid curves – superfluid dynamics approximation given by Eqs. (4)–(6).

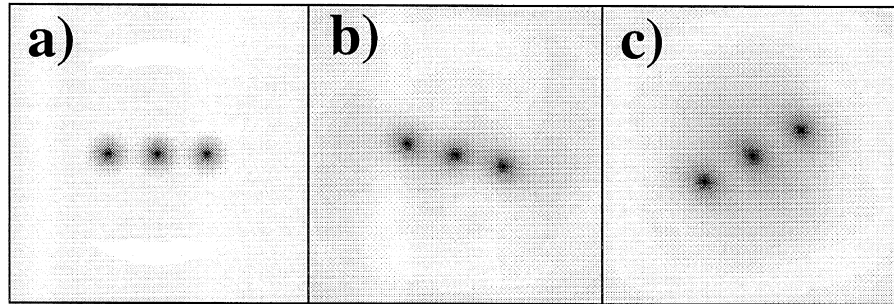


Fig. 3. Grayscale images of the linear structure of three OVSs; (a) at $z = 0L_{NL}$; (b), (c) at $z = 10L_{NL}$, for different topological charge (TC) of the central OVS: (b) $m_c = -1$, (c) $m_c = +1$. The offset between the side-lying vortices is $\Delta = 10.0$. For better visualisation 6.25% of the all computational area is presented.

following relations for the angular velocity of such structures:

$$\frac{d\theta}{dz} = \gamma \frac{3m}{\Delta^2}, \quad (5)$$

for OVSs situated in an equilateral triangle or in a square, and

$$\frac{d\theta}{dz} = \gamma \frac{5m}{2\Delta^2}, \quad (6)$$

for OVSs situated in the apices of a hexagon.

In Fig. 2 we present the dependence of the rotation angle θ versus normalized nonlinear propagation path-length z for ordered structures consisting of N OVSs: a vortex pair, three vortices disposed in an equilateral triangle, four vortices ordered in a square and six vortices forming a hexagon. All OVSs are assumed to be of unit circulations. The distance between each two neighbouring vortices is $\Delta = 7.5$. One can find a good agreement with Eqs. (4)–(6) (solid lines in Fig. 2). The linearity of the dependence shows that the velocity of the rotation is constant. However, when the plane wave background beam (Eq. (2)) is not wide enough, it is found that the depen-

dence of the angular velocity ($d\theta/dz$) on the nonlinear path-length decreases monotonically, due to the background beam self-broadening, influencing the intensity dependent phase distribution [30]. This fact is responsible for the deviations of the numerical points from the superfluid dynamics approximation (solid lines calculated by Eqs. (4)–(6)) at the larger propagation distances ($z > 8L_{NL}$). The simultaneous reverse of the sign of the TC of all OVSs results in a change of the direction of the ensemble rotation only.

Our further analyses are directed toward the investigation of stable ensembles of OVSs, when they are formed at relatively large distances from one another (fluid dynamics approximation). The simplest structure symmetrical in both the TC distribution and the OVSs mutual disposition is the linear one consisting of three OVSs, when an additional vortex is nested in the middle of the vortex pair (Fig. 3a; the offset between the side-lying vortices is $\Delta = 10.0$). If the TC of the central (“control”) OVS is opposite to the TCs of the other ones, one can observe clockwise rotation up to an angle of $\theta = 12^\circ$ at $z = 10L_{NL}$ (Fig. 3b). It is qualitatively the same rotation, like in the case of a vortex pair of $\Delta = 10.0$, but in opposite direction (where $\theta = 11^\circ$,

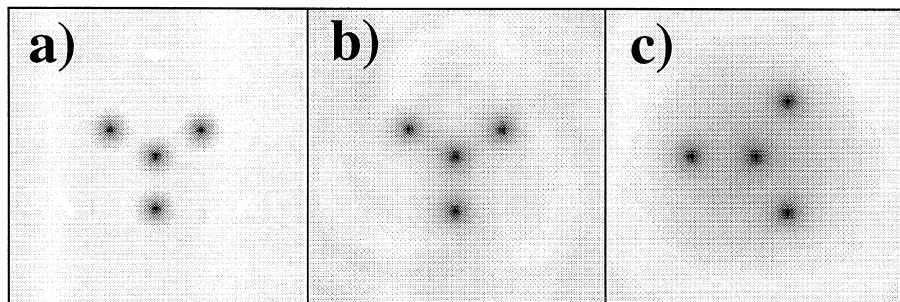


Fig. 4. Grayscale images of the vortex ensemble consisting of three OVSs situated in equilateral triangle; (a) at $z = 0L_{NL}$; (b), (c) at $z = 10L_{NL}$ and for $m_c = -1$ and $+1$ respectively. The offset between the neighbouring OVSs is $\Delta = 10.0$. For better visualisation 6.25% of the all computational area is presented.

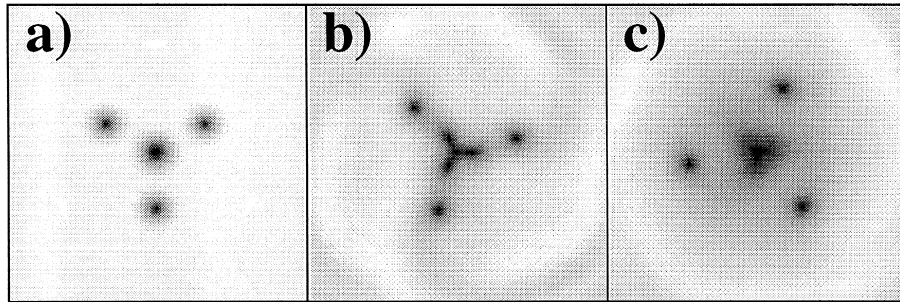


Fig. 5. Grayscale images of the same ensemble pattern like in Fig. 4 but with TC of the central OVS with magnitude of two; (a) at $z = 0L_{NL}$; (b), (c) at $z = 10L_{NL}$ and $m_c = -2, +2$ respectively.

see Fig. 1). Alternating the TC of the central vortex to be equal to the TCs of the other two, one can observe accelerated counterclockwise rotation. The angle of rotation is found to be $\theta(z = 10L_{NL}) = 30^\circ$ (see Fig. 3c), which is about three times larger than the angle of rotation of the vortex pair. In summary, the velocity of rotation of a vortex pair is opposite to that of a vortex ensemble, when the vortex with $m_c = -1$ is nested in the centre of the pair and is three times smaller than the angular velocity of a vortex ensemble with the TC of the central vortex $m_c = +1$. In this way the above results are in good agreement with Eq. (3), describing the vortex motion in the frame of fluid dynamics [2].

In the next step in the analysis we attempted to stabilize the rotation of an ensemble of three OVSs forming an equilateral triangle. As mentioned, such an ensemble rotates axially (Fig. 2, triangles) along the nonlinear path of propagation in agreement with Eqs. (3), (5). Imposing an additional fourth OVS of an opposite TC at the centre of the ensemble (Fig. 4a) we succeed to cancel the rotation (Fig. 4b) during the propagation. The symmetry of this structure, results in simultaneous suppression of the motion within the ensemble. In the absence of an outer circular boundary, the equilibrium frequency of the 2D point vortices forming such an ensemble is zero (see Eq. (7) in Ref. [24]). Substituting the parameters of the considered configuration in Eq. (3) one can obtain that the velocity of each vortex is zero, independent of the particular offset Δ . The latter was proved numerically. In all cases, for different separations between OVSs numerically simulated, no rotation and movement of the OVSs within the ensemble is observed. Only the self-defocusing of the finite extent background beam results in weak increase of the distances between the dark beams. These results could be regarded as additional evidences for the similarity of the motion of the OVSs and vortex lines in hydrodynamics. We tested the stability of this configuration by changing the position of one of the vortices by 0.2Δ . No rotation in the unadjusted structure is observed, and slight movement of the vortices, pronouncing the tendency for restoring the ensemble symmetry is present only.

When the vortex in the ensemble centre (Fig. 4a) has the same TC as the other three OVSs, the rotation speed was found to increase significantly but the relative disposition of the dark beams remains undisturbed (Fig. 4c, where $m_c = +1$, $\theta(z = 10L_{NL}) = 19^\circ$). If the central (“control”) OVS has a higher TC (Fig. 5a) one can force either clockwise rotation (Fig. 5b, where $m_c = -2$, $\theta(z = 10L_{NL}) = 17^\circ$) or counterclockwise rotation of an increased velocity (Fig. 5c, where $m_c = +2$, $\theta(z = 10L_{NL}) = 39^\circ$). These data agree qualitatively well with the analytical results from Ref. [24] (Eq. (7)), in which the rotation reversal of the ensemble leads to a sign-change of the pattern equilibrium frequency.

Generally such an interaction configuration may appear useful for future switching applications based on OVSs. The real utilization of devices based on vortices of higher TCs seems to be embarrassed by their decay into vortices with unit circulations (Figs. 5b, 5c) and probably will be restricted to potential short distance high capacity switching applications.

Further we considered a more complicated configuration, namely four OVSs situated in the apices of a square.

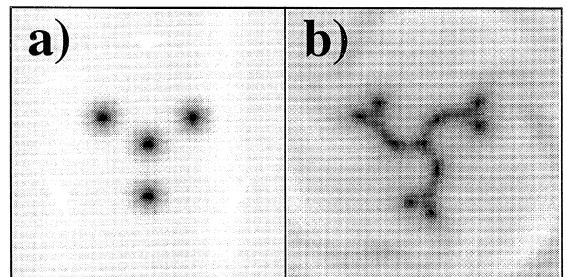


Fig. 6. Grayscale images of the same ensemble pattern like in Fig. 4 but with TCs of the vortices with magnitude of two; (a) at $z = 0L_{NL}$; (b) evolution ensemble of (a) at $z = 10L_{NL}$. A pattern similar to that of the infinite hexagonal lattice is formed. For better visualisation 6.25% of the all computational area is presented.

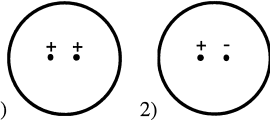
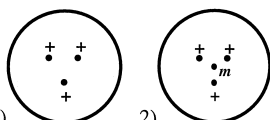
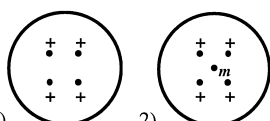
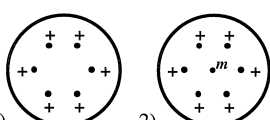
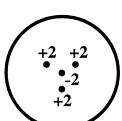
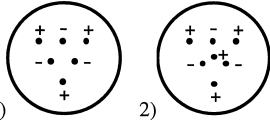
Such configuration is referred to as an ‘‘optical leopard’’ [23], when it consists of alternating positive and negative charged vortices. The nonlinear evolution of this configuration is well described in Ref. [9]. It has been found there that if such an ensemble is considered as consisting of two vortex pairs (with zero total TC), after some nonlinear propagation distance the two effective pairs exchanged their ‘‘partners’’. In this way it has been shown [9] that the coherent interactions of OVSs is elastic. In our investigation we consider the nonlinear propagation of four vortices with equal TCs. As seen in Fig. 2 (squares) such an ensemble rotates continuously and the angle of rotation is described adequately by Eq. (5). We succeed to control this rotation by positioning an additional OVS at the ensemble centre. When the ‘‘control’’ OVS, nested in, is of a TC opposite to that of the other four ones, counter-

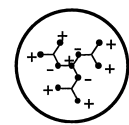
clockwise rotation at an angle $\theta = 4^\circ$ is observed at $z = 10L_{NL}$. The increase of TC of the central OVS to -2 results in a clockwise rotation (reversed in direction) at an angle $\theta = 6^\circ$ (at $z = 10L_{NL}$), in spite of the decay of the central OVS due to modulational instability. When the central OVS has a TC equal to that of the other four ones (i.e. $m_c = +1$), accelerated counterclockwise rotation at $\theta = 25^\circ$ occurs after nonlinear propagation path-length $z = 10L_{NL}$. When the TC of the central OVS is $m_c = +2$, the counterclockwise rotation becomes even stronger ($\theta = 33^\circ$ at $z = 10L_{NL}$). Again, breaking of the central OVS into OVSs with unit circulation occurs.

In order to find other stable configurations of OVSs, different from these presented in Fig. 4b, we investigated the nonlinear propagation of more complicated ordered systems. A pure hexagon ordered ensemble, consisting of

Table 1

Schemes and brief descriptions of all OVS interactions discussed in Section 3 and their characteristic behaviour. In the last row two additional configurations are presented. All numerical simulations are made when the OVS ensemble is superimposed on a finite super-Gaussian background beam at $w = 48.0$ (see Eq. (2)) and at offsets $\Delta = 10.0$

Starting pattern at $z=0L_{NL}$	Observed behaviour (up to $z=10L_{NL}$)
	1) Counterclockwise rotation of the vortex pair around the beam centre. See Fig.2 2) Moving of the vortex pair away from the beam centre
	1) Counterclockwise rotation of the vortex ensemble around the beam centre. See Fig.2 2) Rotation of the ensemble, which can be controlled by changing the TC of the central vortex. Stabilization at $m_c = -1$
	1) Counterclockwise rotation of the vortex ensemble around the beam centre. See Fig.2 2) Rotation of the ensemble, which can be controlled by changing the TC of the central vortex.
	1) Counterclockwise rotation of the vortex ensemble around the beam centre. See Fig.2 2) Rotation of the ensemble, which can be controlled by changing the TC of the central vortex.
	Decay of vortices with higher order TCs and formation of an vortex ensemble pattern, similar to a cell of infinite vortex lattice. See scheme at the right and Fig.7b
	1) Clockwise rotation at $\theta(z=10L_{NL})=29^\circ$ 2) Formation of an vortex ensemble pattern similar to the part of infinite vortex lattice



OVSs of unit TCs, was found to rotate continuously with an angle of rotation well described by Eq. (6) (see also Fig. 2) and equal to 14° at $z = 10L_{\text{NL}}$ and $\Delta = 10.0$. Decreasing of the rotation speed is reached when an OVS with a TC opposite to that of the other OVSs, is nested in the ensemble centre. In this case the angle of rotation was reduced down to $\theta(z = 10L_{\text{NL}}) = 8^\circ$ (counterclockwise). Further reduction of the rotation velocity is reached when the “control” OVS with $m_c = -2$ is nested in the centre. In this way the angle of rotation is found to be minimal for the hexagon-symmetrical configuration $\theta(z = 10L_{\text{NL}}) = 3^\circ$ (counterclockwise). When the TC of the central vortex is $m_c = -3$ the angle of rotation is again $\theta(z = 10L_{\text{NL}}) = 3^\circ$, but the direction of the rotation is reversed (clockwise). According to Eq. (7) from Ref. [24], the equilibrium frequency of an ensemble of point vortices with the same spatial distribution and charges agrees nearly quantitatively (within 20%) with the above data. Again, breaking of the central multiple charged OVS into OVSs with unit circulations was observed in the simulations.

All numerical results presented above are in good agreement with the vortex motion described in superfluid dynamics by Eq. (3). Calculating the velocity of rotation given by this equation we estimate that when the TC of the central vortex is 0, 1, 2 or 3 the velocity is proportional to $5/\Delta$, $3/\Delta$, $1/\Delta$ or $-1/\Delta$, respectively, where Δ is the distance between the neighbouring vortices. It is the same relation like the angles of rotation at $z = 10L_{\text{NL}}$ (which is $14^\circ:8^\circ:3^\circ: -3^\circ$). In this way one could choose the desired discrete rotation by positioning the properly charged “control” OVS (calculated from Eq. (3)) in the centre of the ensemble. The difficulty in the applicability of these results is caused mainly by the break-up of the multiple charged OVSSs. One can construct a practically applicable device when the nonlinear propagation path-length is shorter than the characteristic length of the breaking of these modulationally-unstable solitons. Otherwise the “control” OVS could not be used as an information carrying channel.

The series of numerical simulations presented above show only one stable and stationary symmetrical configuration (Fig. 4b). Following the analogy with superfluid dynamics, for increased magnitude of TC of all the OVSs in this configuration one can expect evolution into another stationary configuration (Fig. 6a). When higher order TCs are nested in a similarly shaped ensemble, the stability should be expected to be poor. Again break-up of the OVSs with TC larger than unity should occur. One can expect that after the complete decay of these OVSs, a stable and stationary ensemble will be formed. In Fig. 6b a grayscale image of such an ensemble consisting of OVSSs with TCs equal to two is shown. As seen, all multiple charged OVSs have decayed into fundamental OVSs. The interesting feature here is that the ensemble pattern in Fig. 6b is very similar to a piece of an infinite hexagonal crystal lattice, consisting of positive and negative OVSs. Following the physical intuition we came to the idea that regular vortex lattices situated on a finite-background beam can propagate stable and rigidly along the NLM. The results of the investigation of the propagation of such a kind of structures are presented in Section 4.

For better understanding of the results presented above, all discussed OVS interactions within the ensembles and some additional ones are summarized in Table 1.

4. Optical vortex soliton lattices composed on finite background beams

Vortex lattices are known in fluid dynamics and they were found to exhibit elasticity and rigidity [2,24]. Some results on the nonlinear propagation of vortices in the form of OVS-lattices are presented in Ref. [7]. In this work the main assumption is that an infinite squared vortex lattice is superimposed on a planewave background. In contrast, in our investigation we set a vortex lattice on a finite background beam and found some characteristic differences in its nonlinear evolution.

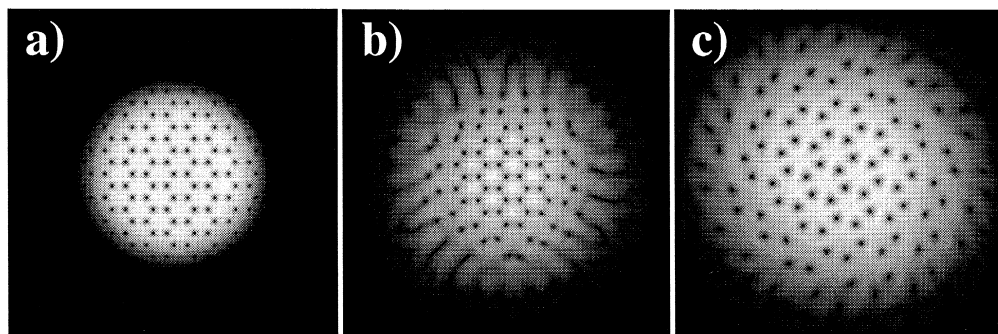


Fig. 7. Grayscale images of the hexagonal vortex lattice; (a) at $z = 0L_{\text{NL}}$; (b), (c) at $z = 10L_{\text{NL}}$. (b) The lattice consists of vortices with alternating unit TCs (zero total TC) and (c) the lattice consists of vortices with equal unit TCs. The offset between the OVSs is $\Delta = 5.0$.

Following the results presented in Fig. 6b we investigate the nonlinear evolution of a hexagonal vortex lattice (Fig. 7a) in a NLM. If it consists of neighbouring OVSs of unit and alternatively changing TCs, it demonstrates well pronounced stable nonlinear propagation (Fig. 7b). Only the background beam spreads due to the self-defocusing nonlinearity, influencing the position of the outer-lying OVSs. If the lattice is composed of vortices with equal TCs the whole ensemble rotates continuously (at the angle $\theta = 40^\circ$ counterclockwise at $z = 10L_{\text{NL}}$; Fig. 7c). In addition, the background beam was found to spread much more intensively than in the case presented in Fig. 7b. The spreading was also substantially stronger compared to that of the smooth background-beam under the same self-defocusing conditions (i.e. when no OVSs are nested in the host beam). The beam intensity was found to decrease rapidly to $0.4I_0(z=0)$ at $z = 10L_{\text{NL}}$.

Similar evolution is found for a square lattice of OVSs superimposed on a finite extent background beam. When all OVSs have equal TC $m = 1$, the rotation of the lattice at $\theta(z = 10L_{\text{NL}}) = 51^\circ$ (counterclockwise) occurs with a corresponding decrease of the maximum intensity of the background to $0.4I_0(z=0)$ level at $z = 10L_{\text{NL}}$. On the contrary, in the case with alternatively changed TCs ($|m| = 1$ and zero total charge), no lattice rotation is observed.

We tested the stability and elasticity of the lattices composed of OVSs (with total TC equal to zero) by shifting one of the OVS out of its equilibrium position. Well expressed stability for all kind of lattices is observed. Slight motion of the shifted OVS and its neighbours, similar to the elasticity motion in a regular crystal lattice is evident. Unfortunately, with the grid mesh used and the maximum propagation path-length reached, we could not surely prove the full elasticity of the OVS lattice. Because of that we shifted a whole row of OVSs in the square-shaped lattice. This test indicates much more clear OVS-row movement and interaction-elasticity.

In conclusion to this section we have to note that OVS-lattices with zero total TC, imposed on a finite-extent background beam can be used for obtaining stable arrays of induced waveguides. Such stationary vortex patterns may also be found useful for suppressing the modulational instability of the planewave background in media with second order nonlinearity (see for example Ref. [36]).

5. Conclusion

Qualitatively, the possibility to control and stabilize (at least partially) ensembles of OVSs against rotation and translation by a proper choice of the topological charge of a “control” OVS nested in the ensemble centre is proved numerically.

Since the terms driving the OVSs motion [25] are the intensity and the phase gradients, by choosing the interme-

diated distance between the OVSs and the width of the background beam to be large enough, the only term responsible for the transverse motion accounts for the phase gradient. In this way it is shown that the motion of the vortex ensemble is adequately described by the Kelvin law in fluid dynamics. On its basis relations describing the vortex motion in regular ordered structures are obtained, which depend on the positions of the vortices and their topological charges. Small deviations from this relation are obtained for larger propagation distances. They are caused by significant spreading of the finite super-Gaussian background beam at these distances.

Positioning an OVS with a certain TC in the ensemble centre (namely in the centre of the rotation, where the phase gradient appears to be zero) influences only the ensemble rotation and keeps the mutual OVS's disposition unchanged.

An extension of the vortex ensembles in regular lattices is analysed. Lattices composed of OVSs with individually alternatively changing TCs corresponding to a total TC equal to zero, are found to be stable.

Acknowledgements

The authors are grateful to the CEEPUS program (Network A21). D.N., A.D. and S.D. thank the Technical University of Graz, Institute of Experimental Physics, for the warm hospitality during their research stay and for the possibility of experimentally proving some of the obtained results. A.D. would like to thank the Alexander-von-Humboldt Stiftung for the possibility to complete this analysis in the fruitful atmosphere of the Max-Planck-Institut für Quantenoptik (Garching, Germany). This work was partially supported by the National Science Foundation, Bulgaria.

References

- [1] J.F. Nye, M.V. Berry, Proc. R. Soc. London A 336 (1974) 165.
- [2] E.B. Sonin, Rev. Mod. Phys. 59 (1987) 87, and references therein.
- [3] R.W. Griffiths, E.J. Hopfinger, J. Fluid Mech. 198 (1987) 73.
- [4] R.G. Creswick, H.L. Morrison, Phys. Lett. A 76 (1980) 267.
- [5] E.M. Wright, R.Y. Chiao, J.C. Garrison, Chaos Solitons Fractals 4 (1994) 1797.
- [6] K.T. Gahagan, G.A. Swartzlander Jr., Optics Lett. 21 (1996) 827.
- [7] G.S. McDonald, K.S. Syed, W.J. Firth, Optics Comm. 94 (1992) 469.
- [8] G.A. Swartzlander Jr., C.T. Law, Phys. Rev. Lett. 69 (1992) 2503.
- [9] K. Staliunas, Chaos, Solitons Fractals 4 (1994) 1783.
- [10] J. Christou, V. Tikhonenko, Yu. Kivshar, B. Luther-Davies, Optics Lett. 21 (1996) 1649.

- [11] P. Coullet, L. Gil, F. Rocca, *Optics Comm.* 73 (1989) 403.
- [12] M.W. Beijersbergen, R.P.C. Coerwinkel, M. Kristensen, J.P. Woerdman, *Optics Comm.* 112 (1994) 321.
- [13] M.W. Beijersbergen, L. Allen, H.E.L.O. van der Veen, J.P. Woerdman, *Optics Comm.* 96 (1993) 123.
- [14] D.V. Petrov, F. Canal, L. Torner, *Optics Comm.* 143 (1997) 265.
- [15] N.R. Heckenberg, R. McDuff, C.P. Smith, A.G. White, *Optics Lett.* 17 (1992) 221.
- [16] B. Luther-Davies, R. Powles, V. Tikhonenko, *Optics Lett.* 19 (1994) 1816.
- [17] G.S. McDonald, K.S. Syed, W.J. Firth, *Optics Comm.* 95 (1993) 281.
- [18] C.T. Law, G.A. Swartzlander Jr., *Optics Lett.* 18 (1993) 586.
- [19] D.E. Pelinovsky, Y.A. Stepanyants, Yu.S. Kivshar, *Phys. Rev. E* 51 (1995) 5016.
- [20] A.W. Snyder, L. Poladian, D.J. Mitchell, *Optics Lett.* 17 (1992) 789.
- [21] C.T. Law, G.A. Swartzlander Jr., *Chaos, Solitons Fractals* 4 (1994) 1759.
- [22] G. Indebetouw, *J. Mod. Optics* 40 (1993) 73.
- [23] C.O. Weiss, H.R. Telle, K. Staliunas, M. Brambilla, *Phys. Rev. A* 47 (1993) R1616, and references therein.
- [24] I.M. Lansky, T.M. O’Neil, *Phys. Rev. E* 55 (1997) 7010, and references therein.
- [25] D. Rozas, C.T. Law, G.A. Swartzlander Jr., *J. Opt. Soc. Am. B* 14 (1997) 3054.
- [26] D. Rozas, Z.S. Sacks, G.A. Swartzlander Jr., *Phys. Rev. Lett.* 79 (1997) 3399.
- [27] L. Gil, K. Emilsson, G.-L. Oppo, *Phys. Rev. A* 45 (1992) R567.
- [28] F. Lund, *Phys. Lett. A* 159 (1991) 245.
- [29] I. Velchev, A. Dreischuh, D. Neshev, S. Dinev, *Optics Comm.* 130 (1996) 385.
- [30] Y. Kivshar, X. Yang, *Optics Comm.* 107 (1994) 93.
- [31] I. Velchev, A. Dreischuh, D. Neshev, S. Dinev, *Optics Comm.* 140 (1997) 77.
- [32] I. Aranson, V. Steinberg, *Phys. Rev. B* 53 (1996) 75.
- [33] I.V. Basistiy, V.Yu. Bazhenov, M.S. Soskin, M.V. Vashnetsov, *Optics Comm.* 103 (1993) 422.
- [34] A.V. Mamaev, M. Saffman, A.A. Zozulya, *Phys. Rev. Lett.* 78 (1997) 2108.
- [35] D. Neshev, A. Dreischuh, V. Kamenov, I. Stefanov, S. Dinev, W. Fließner, L. Windholz, *Appl. Phys. B* 64 (1997) 429.
- [36] A.V. Buryak, Yu.S. Kivshar, *Optics Lett.* 20 (1995) 834.